Journal of Alloys and Compounds 495 (2010) 341–344

Contents lists available at ScienceDirect

Journal of Alloys and Compounds

journal homepage: www.elsevier.com/locate/jallcom

Deformation kinetics of Zr-based bulk metallic glasses—Temperature and strain rate influences on shear banding

Florian H. Dalla Torre*, Alban Dubach, Jörg F. Löffler

Laboratory of Metal Physics and Technology, Department of Materials, ETH Zurich, Wolfgang-Pauli-Str. 10, 8093 Zurich, Switzerland

ARTICLE INFO

Article history:
Received 6 August 2008
Received in revised form 5 October 2009
Accepted 6 October 2009
Available online 13 October 2009

Keywords:
Bulk metallic glass
Deformation kinetics
Activation volume
Shear banding
Inhomogeneous flow

ABSTRACT

At low homologous temperatures metallic glasses exhibit inhomogeneous flow behaviour, which is associated with narrow shear banding. Based on the width of the shear bands and the time-dependent heat conduction, we show here that this process is not fully adiabatic at low strain rates, even though temperatures are sufficiently high to create a drop in viscosity within either a new or a pre-existing shear band. Evaluation of the deformation kinetics at cryogenic temperatures suggests an increase in viscosity within the shear band, although temperatures are still sufficiently high to cause localised melting at fracture. In addition, a change from serrated to non-serrated flow can be observed if the temperature is lowered below a critical value. This macroscopic change in the flow behaviour is directly related to a change in the strain rate sensitivity from negative to positive values, suggesting a clear change in deformation behaviour. We propose a refined shear dilatation model to explain the experimental findings.

1. Introduction

Shear banding in coarse-grained 'hard-to-deform' metals typically occurs under dynamic loading, where micrometer-wide shear bands result [1]. However, reducing grain size in metals which in their coarse-grained state are regarded as being 'soft' also generates a gradual shift in their affinity to deform via shear banding. For example, nanocrystalline Ni exhibits shear bands, while its coarse-grained counterpart does not when tested at room temperature and at strain rates of $10^3\ s^{-1}$ [2,3]. The resulting increase in strength due to grain size reduction actually causes a reduction in strain and strain hardening ability, which is a favourable condition for the initiation of shear localisation, i.e. shear banding even at lower strain rates [4]. This is why the fracture angle of many fractured ultra-fine-grained or nanocrystalline samples tested in tension measures ~45° [5]. The ultimate reduction in grain size generates an amorphous material which, compared to its nanocrystalline counterparts, exhibits strong differences in general physical properties [6–8]. In terms of compressive flow stress, however, it may not behave very differently to a chemically similar crystalline phase with grain sizes on the order of a few tens of nanometers [9]. In the latter case this is related to the restricted activity of dislocation motion, which at very fine grain size ceases and which is accompanied by a marked transition to inhomogeneous, glass-like flow [9], where fracture angles in tension and compression deviate from 45° [10,11]. Shear localisation in metallic glasses, however is more pronounced than in nanocrystalline metals. Only at temperatures close to their glass transition temperature, shear localisation can be avoided if tested at low strain rates [12,13]. In the temperature range where shear banding is present, the deformation kinetics are not yet clearly understood. First, shear bands are significantly thinner than in crystalline metals, on the order of tens of nanometers [14–18]. Second, it is not clear to date if this process is adiabatic or not under quasistatic conditions. And third, it is still arguable as to what the exact deformation mechanisms in BMGs are (ref. [19] and references therein). Apart from the temperature increase during localized shearing, the shear dilatation models (the shear transformation zone (STZ) model [20] and the free volume or diffusive-jump-like model [21–23] have found wide acceptance in explaining the drop in viscosity as also recently reviewed by Schuh et al. [19]. On the other hand, however, none of the constitutive equations for inhomogeneous plastic flow ascribed by these models addresses the serrated flow as a kinetic phenomenon sufficiently well, this partially due to the lack of experimental evidence. In this study we give a detailed description of the deformation behaviour of a Zr-based bulk metallic glass (BMG) deformed at quasi-static conditions at various temperatures in the hope of shedding more light on the deformation of BMGs.

2. Experimental procedure

$Zr_{57.9}Cu_{22}Fe_8Al_{12}Pd_{0.1}$ and $Zr_{52.5}Ti_5Cu_{17.9}Ni_{14.6}Al_{10}$ (Vit105) prealloys were prepared by arc-melting the pure elements (purity > 99.995%) in a Zr-gettered argon atmosphere from which cylindrical rods were suction-cast into a copper mold with

* Corresponding author.
E-mail addresses: florian.dallatorre@mat.ethz.ch, florian.dallatorre@swissmetal.com (F.H. Dalla Torre).

0925-8388/$ – see front matter © 2009 Elsevier B.V. All rights reserved.
doi:10.1016/j.jallcom.2009.10.015

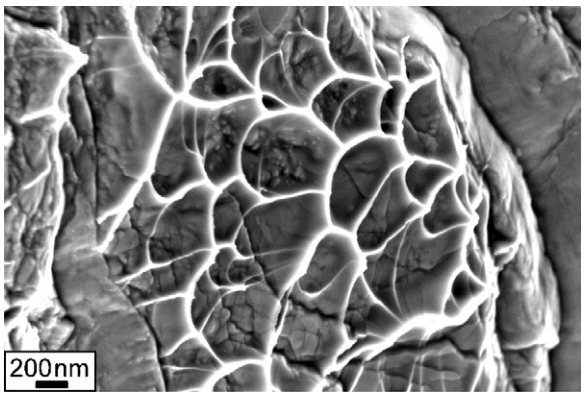

Fig. 1. Viscous flow features on a shear plane of an unfractured compression test sample of $Zr_{57.9}Cu_{22}Fe_8Al_{12}Pd_{0.1}$.

a length of ~30 mm and diameters of 3 and 2 mm, respectively. Compression test specimens with a length-to-diameter ratio of 1.7 were cut from these rods and subsequently polished. The amorphous structure of the specimens was confirmed by means of X-ray diffraction (XRD) using a PANalytical X'pert diffractometer with Cu Kα radiation, and by differential scanning calorimetry (DSC) using a Setaram Labsys DSC. The deformed specimens were examined with a LEO 1530 scanning electron microscope (SEM) equipped with a field emission gun. Constant cross-head displacement tests and strain rate jump tests in compression were performed on a 4-column Schenck-Trebel machine equipped with a 100 kN load cell. Tests were performed at various crosshead velocities ranging from 1.0 to 0.1 mm/min, resulting in initial strain rates of 3×10^{-3} to 3×10^{-4} s^{-1}. The strain was measured from the crosshead displacement and a strain gauge positioned on the pistons above and below the specimen. Acquisition rates of 20–1200 Hz were used to provide information on the shear band velocity.

3. Results and discussion

Fig. 1 shows an SEM image of a sample deformed without fracture which exhibits a shallow viscous-like layer underneath a more brittle structure. This information suggests that even before fracture, sufficiently high temperatures can be reached which yield to viscous flow features. Thickness estimates from this and similar SEM images together with cross-sectional views made by transmission electron microscopy (TEM) suggest that the heat-affected width is restricted to one to two hundred nanometers maximum, and often less. Note that at the moment of fracture, stresses are relieved which are approximately 3 orders of magnitude higher than during shear banding before fracture [24]. Thus at the moment of fracture the viscous layer is a few micrometers thick [24].

Under adiabatic conditions the following expression must be fulfilled:

$$x = \sqrt{\Delta t \alpha}, \quad (1)$$

where x is the width of the heat-affected zone (here taken as the width of a shear band), α is the thermal diffusivity, and Δt is the time needed for this process to occur. Table 1 shows that using Eq. (1) with a diffusivity of 3.2×10^{-6} m^2/s at T_g [25], duration times in the sub-nanosecond range arise for a shear band of 10 nm width, while for a shear band of 100 nm width a few nanoseconds would be required. A width of 5 μm would on the other hand require a few microseconds to heat up this area. There are several approaches to estimating the duration time. All, however, assume that the duration time for the heat burst is the same time span required for the activation of a local shear event (independent of the size of such an event).

Table 1
Values for the width of the heat-affected zone and the time duration calculated according to Eq. (1).

Width of heat-affected zone, x [nm]	Time Δt [ns]
10	0.03
100	3.1
200	12.5
1000	312.5
5000	7812.5

During spatially inhomogeneous flow deformation can also occur in a temporal inhomogeneous manner. This is the case at room temperature and is reflected by a jerky flow or serrated flow curve. Below a critical temperature smooth yielding occurs (temporally homogeneous, but spatially inhomogeneous). Fig. 2a shows two compressive flow curves at room temperature and liquid nitrogen temperature, where the crosshead velocity is changed by one order of magnitude, i.e. where a change in the strain rate between 10^{-3} and 10^{-4} s^{-1} is applied. Fig. 2b shows a detail of the serrated flow curve measured at room temperature. It is characterized by loading parts, which reflect the elastic modulus of the material and by stress drop parts, where plastic deformation via shear banding occurs. Typically the time required for the stress to drop is significantly faster than the loading time of the elastic part. Measuring the duration time of such stress drops at room temperature reveals time scales on the order of a few tens of milliseconds (irrespective of the acquisition speed). Assuming this to be the duration time Δt the thickness of the heat-affected width would be far too large *before* fracture if one assumes adiabatic conditions; however, *at* fracture agreement with the thickness of the viscous-like layer of the fracture surface results.

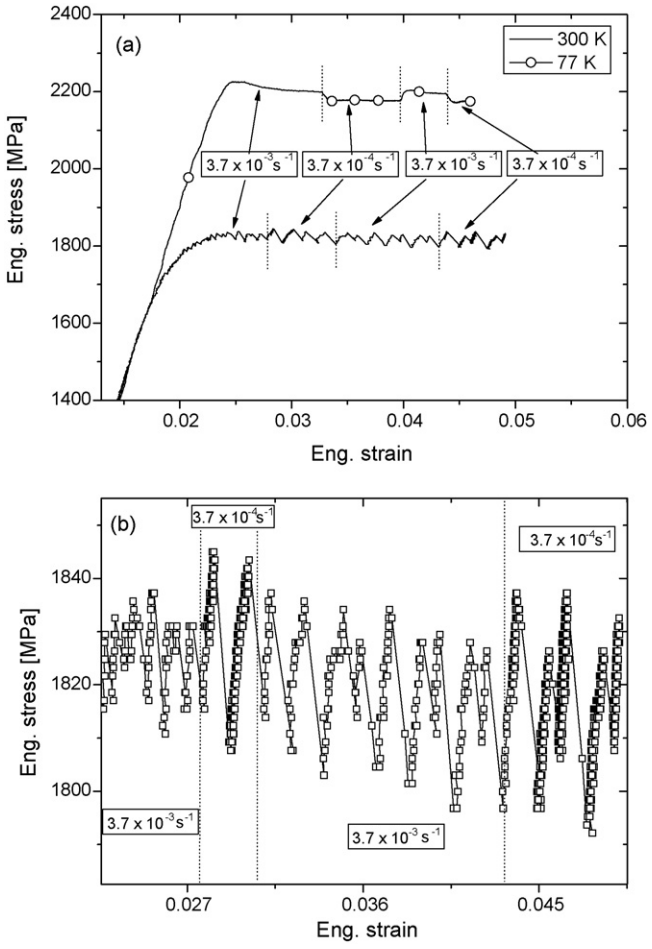

Fig. 2. (a) Stress–strain curve at varying strain rates for $Zr_{57.9}Cu_{22}Fe_8Al_{12}Pd_{0.1}$ measured at room temperature and liquid nitrogen temperature. (b) Detail taken from the curve measured at room temperature, showing the variation of the flow stress on the applied strain rate. Note that each open square represents one data point.

Another way to measure the duration time of a shear event is by acoustic emission, assuming that a shear event generates elastic wave propagation which is audible when exiting the material. In agreement with the work of Vinogradov and Khonik [26], our results show that the smallest measureable events take place within a few microseconds. Again assuming that these time periods reflect the duration time Δt, values of several micrometers width (which are still too large) would result for shear events taking place before fracture.

A third way to estimate Δt is to assume that the shear events that are responsible for adiabatic heating travel through the media at the speed of sound [27]. This would be the utmost limit with the shortest values for Δt. In metals velocities of 3000–6000 m/s are typical; in other words, 90–180 nm per 0.03 ns or 9–18 μm for a 3 ns duration time would be required (taking the values in the first two rows of Table 1, which in terms of x corresponds to the experimentally deduced values of a shear band width). Obviously these are very large shear displacements. Fig. 3 shows details from a stress–displacement curve recorded at room temperature, where displacement bursts of several hundred nanometers to a few micrometers are shown at the onset of plastic yielding and at a later stage, respectively. Recently we were able to show that these displacement bursts can be correlated well in size with shear steps on the shear surface [24]. Thus good agreement results with respect to the shear displacement, assuming a shear event travelling at the speed of sound. However, if we compare the duration time measured for the shear displacement of a stress–strain curve, a large deviation from the duration time calculated in Table 1 results. Thus it is assumed here that adiabatic heating is not entirely fulfilled during shear banding in BMGs. In addition, if equations evaluating the temperature increase within a shear band [24] are taken into account, a discrepancy between values *at* fracture and *before* fracture results. In agreement with current literature [27], [28–30] this suggests that shear localisation is the cause of a temperature increase due to frictional sliding, and not vice versa.

In the following the deformation kinetics of Zr-based BMGs is addressed. The two stress–strain curves produced from the same sample batch shown in Fig. 2 were measured once at 77 K and once at 300 K. The strain rate $\dot{\varepsilon}$ was alternated between $3.7 \times 10^{-3}\ s^{-1}$ and $3.7 \times 10^{-4}\ s^{-1}$. As indicated in Fig. 2 for this alloy, and in more detail for the binary BMG $Cu_{50}Zr_{50}$ and for $Zr_{52.5}Ti_5Cu_{17.9}Ni_{14.6}Al_{10}$ (Vit105) (see also refs. [31–33]), a decrease was measured in the steady-state strain rate sensitivity (SRS), which is defined as

$$m = \left(\frac{\partial \ln\sigma}{\partial \ln\dot{\varepsilon}} \right)_{\varepsilon}, \tag{2}$$

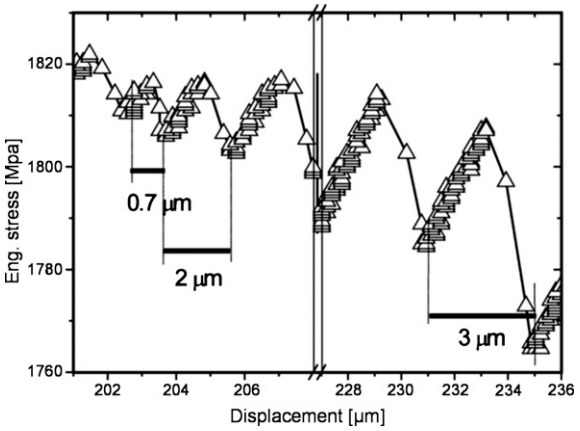

Fig. 3. Typical engineering stress displacement diagram showing the magnitude of a shear displacement associated with a stress drop taken from a compression test on Vit105.

from values of 0.004 at 77 K to values of approximately −0.002 at 300 K. This change in the deformation kinetics strongly suggests a fundamental change in the deformation mechanism. We recently compared the phenomenological similarities of serrated flow behaviour in metallic glasses [31–33] with that of crystalline alloys which show the so-called dynamic strain aging (DSA) effect [34], more commonly known as the Portevin–LeChâtelier phenomenon. In the alloys studied here, we observe a transition, similar to the DSA effect, from negative to positive SRS with decreasing temperature, which accompanies a change from serrated to smooth yielding (Fig. 2). Our results show that shear bands in metallic glasses exhibit a memory of their strain history, which is reflected by the increase in $\Delta\sigma$ and shear displacement with strain (Fig. 3) and the decrease of the SRS at room temperature [32]. In DSA-deforming crystalline alloys such behaviour has been explained by considering the stress relaxation in the vicinity of a shear band [35].

Our micromechanical view of the shear process in BMGs is based on the fact that a shear band represents an energetically unfavourable structural state, which if time and temperature permit will structurally relax spontaneously towards a lower energy state [33]. Based on this, we introduced a state variable (Δg) into the rate equation, which accounts for this dynamical structural change within a shear band, i.e. the shear strain rate is

$$\dot{\gamma} = \dot{\gamma}_0 \exp\left(\frac{-\Delta G}{k_B T}\right) = \dot{\gamma}_0 \exp\left(\frac{-\Delta G_0 + \Delta g(T, \dot{\gamma}, \gamma) - V_{ap}\tau_{eff}}{k_B T}\right), \tag{3}$$

where $\dot{\gamma}_0$ is typically taken as the characteristic strain rate that depends on an attempt frequency and k_B and T are the Boltzmann constant and temperature, respectively. Note that due to the high applied stress, backward fluctuations are unlikely to occur. The Gibbs free energy ΔG required for the process to take place is equal to the difference between the total energy required (total energy barrier, ΔG_0), the energy state variable Δg and the work performed by the effective stress τ_{eff} on a volume V_{ap}. The latter, defined as the apparent activation volume, is

$$V_{ap} = k_B T \left(\frac{\Delta \ln \dot{\gamma}}{\Delta \tau}\right). \tag{4}$$

and can be experimentally measured by strain rate jump or relaxation tests [3]. This quantity can be further related to the volume of a shear transformation zone by $V_{ap} = \Omega_0 \gamma_0$, where γ_0 is the critical strain of a STZ, which is on the order of 0.1 and Ω_0 is the size of a STZ [20]. For Vit105 ($Zr_{52.5}Ti_5Cu_{17.9}Ni_{14.6}Al_{10}$) V_{ap} increases with increasing strain rate from 0.15 to 0.23 nm^3 at 77 K, which for a characteristic shear strain $\gamma_0 \sim 0.1$ [20] yields $\Omega_0 \sim 70$–120 atoms [24,36]. The values deduced here are of the same order of magnitude and accord very well with recent theoretical models and molecular dynamic simulations, where the volume of a STZ has been identified to be in the range of 100–140 atoms [37–39]. In addition to the increase in V_{ap} with increasing strain rate, we also measured an increase of V_{ap} with increasing temperature from 0.15 nm^3 at 77 K to 3.6 nm^3 at 195 K [36]. The variable Δg, which depends on temperature, strain and strain rate, introduces the temporal evolution of the atomic structure (dilatation and structural relaxation) within shear bands *after* a shear event has taken place (i.e. in the absence of effective stress).

Recalling the shear displacement above (Fig. 3 and also Fig. 9 in Ref. [24]) and considering the activation volume measured via strain rate jump tests, a comparison of their magnitudes is now possible. In crystals the activation volume can typically be discriminated into an area a swept by the dislocation segment times the Burgers vector ($V_{ap} = ab$). For simplicity, here the Burgers vector is taken as the average interatomic distance, which for our Zr-based

Table 2
Activation volume and area deduced from strain rate jump tests of Vit105 [33,24,36].

Temperature [K]	Strain rate [s^{-1}]	Activation volume V_{ap} [nm^3]	Activation volume [b^3]	STZ volume Ω_0 [nm^3]	a [nm^2]	l [nm]
77	5×10^{-5}	0.15	44	1.5	0.97	1.11
77	5×10^{-2}	0.23	68	2.3	1.49	1.70
195	5×10^{-5}	3.6	1067	36	23.37	26.6

BMG is on the order of $b \sim 0.154$ nm. The area a can then be further separated into a distance of the shear displacement ξ times the length of the shear transformation zone or (for crystals) dislocation segment l. Assuming a disc-shape STZ volume, similar to an embryonic dislocation loop and taking into account the characteristic shear strain $\gamma_0 \sim 0.1$ as deduced by Argon [20], the following relationship can be obtained:

$$\gamma_0 = 0.1 = \tan\frac{\xi}{b} \Rightarrow \xi = 0.879 \text{ nm} \quad (5)$$

If one assumes ξ to be constant a shear displacement of approximately 5–6 atomic distances is obtained. Note, however, that the shear displacement is more likely to vary with temperature and the stress needed to shear the volume. Table 2 summarises these results and the corresponding dimensions deduced from the activation volumes. These values are, however, roughly 2–3 orders of magnitude smaller when compared with the values deduced from SEM images and the shear steps deduced from Fig. 3, and thus difficult to relate to any microstructurally observable dimension. Therefore it is important here to realise that shear steps associated with a stress drop do not represent one shear event per se, but must correspond to an avalanche of multiple shear events leading to large shear offsets. Similarly and analogously, the activation volume of nanocrystalline metals is of a similar magnitude to the values measured in [36] and discussed here, although shearing resulting in the required shear displacements occurs in a cooperative way. Therefore we consider it unlikely that the activation of shear events is coupled with adiabatic heating; these shear events travel through the material at the speed of sound, creating shear events with shear displacements of hundreds of nanometers or even micrometers.

In the above we have discussed the likelihood of shearing under adiabatic versus non-adiabatic conditions. Based on the results deduced from stress–strain curves measured at various strain rates and temperatures and from microstructural SEM analysis on shear planes, we have demonstrated that that shearing probably occurs in a non-adiabatic fashion (in agreement with current literature [27,28]) and that single shear events a few nanometers in size are activated in a cooperative manner, creating avalanches which lead to shear displacements of several hundred nanometers or a few micrometers.

4. Conclusions

This work summarises recent results obtained for various Zr-based bulk metallic glasses. Detailed analysis of compression curves at various strain rates and temperature reveals a low-temperature regime where deformation is spatially inhomogeneous but temporarily homogeneous, producing non-serrated flow curves and positive strain rate sensitivities. Above a critical strain rate and temperature deformation is spatially and temporarily inhomogeneous and generates a serrated flow curve. An alternative model for deformation kinetics is proposed in which a state variable (Δg) accounts for the structural variation in a shear band, which at sufficiently high temperatures and slow strain rates is prone to structurally relax to a more favourable configuration. Based on mechanical testing and on microstructural information deduced by SEM observations of shear planes before fracture, we suggest that deformation does not occur under adiabatic conditions, but that the heat generated is a cause of flow localisation and frictional effects.

References

[1] Q. Wei, L. Kecskes, T. Jiao, K.T. Hartwig, K.T. Ramesh, E. Ma, Acta Mater. 52 (2002) 1859.
[2] F. Dalla Torre, H. Van Swygenhoven, M. Victoria, Acta Mater. 50 (2002) 3957.
[3] F. Dalla Torre, P. Spätig, R. Schäublin, M. Victoria, Acta Mater. 53 (2005) 2337.
[4] D. Jia, K.T. Ramesh, E. Ma, Acta Mater. 51 (2003) 3495.
[5] M. Dao, L. Lu, R.J. Asaro, J.T.M. De Hosson, E. Ma, Acta Mater. 55 (2007) 4041.
[6] W.L. Johnson, MRS Bull. 24 (1999) 42.
[7] A. Inoue, Acta Mater. 48 (2002) 279.
[8] J.F. Löffler, Intermetallics 11 (2003) 529.
[9] J.R. Trelewicz, C.A. Schuh, Acta Mater. 55 (2007) 5984.
[10] P. Lowhaphandu, S.L. Montgomery, J.J. Lewandowski, Scripta Mater. 41 (1999) 19.
[11] J.J. Lewandowski, P. Lowhaphandu, Philos. Mag. A 82 (2002) 3427.
[12] J. Lu, G. Ravichandran, W.L. Johnson, Acta Mater. 51 (2003) 3429.
[13] A.H. Vormelker, O.L. Vatamanu, L. Kecskes, J.J. Lewandowski, Met. Mater. Trans. A 39 (2008) 1922.
[14] T. Masumoto, R. Maddin, Acta Metall. 19 (1971) 725.
[15] P.E. Donovan, W.M. Stobbs, Acta Metall. 29 (1981) 1419.
[16] E. Pekarskaya, C.P. Kim, W.L. Johnson, J. Mater. Res. 16 (2001) 2513.
[17] J. Li, Z.L. Wang, T.C. Hufnagel, Phys. Rev. B 65 (2002) 144201.
[18] J. Saida, A.D.H. Setyawan, H. Kato, A. Inoue, Appl. Phys. Lett. 87 (2005) 151907.
[19] C.A. Schuh, T.H. Hufnagel, U. Ramamurty, Acta Mater. 55 (2007) 4067.
[20] A.S. Argon, Acta Metall. 27 (1979) 47.
[21] M.H. Cohen, D. Turnbull, J. Chem. Phys. 31 (1959) 1164.
[22] M.H. Cohen, D. Turnbull, J. Chem. Phys. 52 (1970) 3038.
[23] F. Spaepen, Acta Metall. 25 (1977) 407.
[24] F.H. Dalla Torre, A. Dubach, J. Schällibaum, J.F. Löffler, Acta Mater. 56 (2007) 4635.
[25] M. Yamasaki, S. Kagao, Y. Kawamura, Appl. Phys. Lett. 84 (2004) 4654.
[26] A.Yu. Vinogradov, V.A. Khonik, Philos. Mag. 84 (2004) 2147.
[27] J.J. Lewandowski, A.L. Greer, Nat. Mater. 5 (2006) 15.
[28] Y. Zhang, N.A. Stelmashenko, Z.H. Barber, W.H. Wang, J.J. Lewandowski, A.L. Greer, J. Mater. Res. 22 (2007) 419.
[29] T.H. Hufnagel, T. Jaiao, Y. Li, L.-Q. Xing, K.T. Ramesh, J. Mater. Res. 17 (2002) 1441.
[30] W.J. Wright, R.B. Schwarz, W.D. Nix, Mater. Sci. Eng. A 319–321 (2001) 229.
[31] F.H. Dalla Torre, A. Dubach, M.E. Siegrist, J.F. Löffler, Appl. Phys. Lett. 89 (2006) 091918.
[32] F.H. Dalla Torre, A. Dubach, A. Nelson, J.F. Löffler, Mater. Trans. 48 (2007) 1774.
[33] A. Dubach, F.H. Dalla Torre, J.F. Löffler, Philos. Mag. Lett. 87 (2007) 695.
[34] R.A. Mulford, U.F. Kocks, Acta Metall. 27 (1979) 1125.
[35] J.M. Robinson, M.P. Shaw, Int. Mater. Rev. 39 (1994) 113.
[36] A. Dubach, F.H. Dalla Torre, J.F. Löffler, Acta Mater. 75 (2009) 881.
[37] W.L. Johnson, K. Samwer, Phys. Rev. Lett. 95 (2005) 195501.
[38] M. Zink, K. Samwer, W.L. Johnson, S.G. Mar, Phys. Rev. B 73 (2006) 172203.
[39] S.G. Mayr, Phys. Rev. Lett. 97 (2006) 195501.